# Detection of X-ray galaxy clusters based on the Kolmogorov method[(a)]

V.G. Gurzadyan[1], F.Durret[2,3], T. Ghahramanyan[1], A.L. Kashin[1], H.G. Khachatryan[1] and E. Poghosian[1]

1. Alikhanian National Laboratory and Yerevan State University, Yerevan, Armenia; 2. UPMC Université Paris 06, UMR 7095; 3. Institut d'Astrophysique de Paris, F-75014, Paris, France

**Abstract.** - The detection of clusters of galaxies in large surveys plays an important part in extragalactic astronomy, and particularly in cosmology, since cluster counts can give strong constraints on cosmological parameters. X-ray imaging is in particular a reliable means to discover new clusters, and large X-ray surveys are now available. Considering XMM-Newton data for a sample of 40 Abell clusters, we show that their analysis with a Kolmogorov distribution can provide a distinctive signature for galaxy clusters. The Kolmogorov method is sensitive to the correlations in the cluster X-ray properties and can therefore be used for their identification, thus allowing to search reliably for clusters in a simple way.

**Introduction.** – The reliable determination of galaxy clusters as entities is crucial not only for the studies of their individual structure and evolution, but in the broader context of the formation of large scale structures in the universe. Various methods to define the cluster membership of galaxies have been developed, usually based on limited information such as line-of-sight velocities or photometric redshifts (1D), and coordinates (2D). X-ray imaging has provided an important means to detect clusters as diffuse X-ray sources and to define cluster properties by allowing to derive their overall gravitational potential, including dark matter, under the assumption that the X-ray emitting gas is in hydrostatic equilibrium in the cluster gravitational potential well dominated by dark matter.

In the present paper we apply the Kolmogorov stochasticity parameter method and distribution [1,2] to analyze X-ray data, in order to reveal possible signatures which can allow to identify a galaxy cluster. This approach quantifies the degree of randomness for given sequences of numbers and has been applied to various systems appearing in number theory [3,4]. We have also applied this method to the cosmic microwave background (CMB) radiation signal [5,8]. It allowed to identify non-Gaussianities in the

CMB such as the Cold Spot in the maps of the Wilkinson Microwave Anisotropy Probe (WMAP). The behavior of the stochasticity parameter supports the void nature of that anomaly, and another non-Gaussianity, the North Cold spot, has also been identified in the north sky by the same method [6]. This approach was also efficient at detecting point sources in the WMAP maps, including the prediction [7] of gamma-ray sources (quasars, blazars) which have later been identified by the Fermi satellite [9].

Much has been learnt these past ten years on the properties of X-ray clusters, based on the data acquired by the XMM-Newton, Chandra and Suzaku satellites, and the corresponding references are too numerous to be quoted here (for overview see e.g. NASA and ESA sites for X-ray missions **http://www.nasa.gov/missions/index.html; http://www.esa.int/esaSC**). In particular, with its large collecting area, XMM-Newton has allowed not only to draw accurate emissivity maps, but also to compute hardness ratio, temperature and metallicity maps of the X-ray gas (as first obtained by [10,11]). These maps give a much deeper insight on the cluster properties, in particular on the cluster merging history. They have shown unambiguously that even clusters with X-ray emissivity maps showing a relatively relaxed appearance could in fact be undergoing one or several mergers (see e.g. [12] and references therein). Several cluster surveys

---

[(a)]Based on observations obtained with XMM-Newton, an ESA science mission with instruments and contributions directly funded by ESA Member States and NASA

based on XMM-Newton data are available, the first being those of [13–15]. The XMM-Newton archive is now extremely large, and a simple method applied to detect clusters throughout this archive would be a very powerful tool to obtain a large and homogeneous sample of clusters. Note that presently very large and homogeneously detected cluster catalogs are also being obtained, based on the Sunyaev-Zel'dovich effect, both with ground based facilities such as the South Pole Telescope [16] or the Planck satellite [17].

The aim of the present study is not to analyse the properties of individual clusters, but to show that the Kolmogorov descriptor, considered as a quantifier of correlations in datasets, can be used for the identification of galaxy clusters based on X-ray data. For this particular aim we will use a sample of Abell clusters with available XMM-Newton data.

The paper is structured as follows: we briefly describe our method in Section 2, we present our sample of X-ray clusters and analysis together with our results in Section 3. Conclusions are drawn in Section 4.

**The method.** – The definition of the Kolmogorov stochasticity parameter [1,2] is given for a finite random sequence of real numbers $x_1, x_2, \ldots, x_n$ so that the values of $x_n$ are sorted in an increasing manner: $x_1 \leq x_2 \leq \ldots \leq x_n$.

One can define an empirical distribution function:

$$C_n(X) = (number\, of\, the\, elements\, x_i \leq X),$$

where

$$C_n(X) = \begin{cases} 0, & X < x_1 \\ k/n, & x_k \leq X < x_{k+1} \\ 1, & x_n \leq X \end{cases} \quad (1)$$

The theoretical distribution function $C(X)$ is then:

$$C(X) = n \cdot (probability\, of\, the\, event\, x \leq X).$$

The stochasticity parameter $\lambda_n$ for a sequence of $n$ values of $x$ is defined as:

$$\lambda_n = sup_X |C(X) - C_n(X)|/\sqrt{n}. \quad (2)$$

According to Kolmogorov's theorem, $\lambda_n$ is a random number with an empirical distribution function

$$\Phi_n(\Lambda) = (number\, of\, elements\, \lambda_n \leq \Lambda),$$

uniformly converging to $\Phi(\Lambda)$ at $n \to \infty$ for any continuous distribution $C(X)$

$$\Phi_n(\Lambda) \to \Phi(\Lambda), \quad (3)$$

where

$$\Phi(\Lambda) = \sum_{k=-\infty}^{+\infty} (-1)^k e^{-2k^2\Lambda^2}, \quad -\infty < k < +\infty. \quad (4)$$

The distribution function $\Phi(\Lambda)$ varies monotonically from $\Phi(0) = 0$ to $\Phi(\infty) = 1$.

According to the definition, for large enough $n$ and random sequence $x_n$ the Kolmogorov stochasticity parameter $\lambda_n$ will have a distribution close to $\Phi(\Lambda)$. If the sequence is not random, the distribution will be different. So $\Phi(\Lambda)$ denotes a quantitative measure for the randomness of a sequence. Arnold has shown the informativity of this method already for sequences of n=15 [2].

**Analysis and results.** – Our analysis is based on a sample of 40 Abell clusters with data available in the second XMM-Newton Serendipitous Source Catalogue, 2XMM, released on April 15, 2010: the 2XMMi-DR3 catalogue[1] in the [0.2-12] keV band, of median flux $2.5\,10^{-14}$ erg cm$^{-2}$ s$^{-1}$. The X-ray images of the clusters represent datasets of X-ray fluxes for pixels with given coordinates. Table 1 shows the relevant data for the 40 clusters; the first 17 have redshifts lower than 0.03, although no noticable redshift dependence have been noticed at the study below. For illustration in **Figure 1 we represent the X-ray image** for a particular cluster, A2870, and in Figure 2 the cuts of its X-ray flux distribution over the Galactic $l$ and $b$ coordinates.

We then create Gaussian mocks of the clusters, **namely, the mock of a given cluster is obtained as a Gaussian distribution of the flux with the median and standard deviation defined by the real data of its X-ray pixelized distribution**; the cuts along two axes are also shown in Figure 2. Since the Gaussian mocks of the clusters cannot possess the information on the cluster potential carried by the real X-ray images, they can serve as a calibration for the correlations in the real data, i.e. what we have to quantify using Kolmogorov's method. Comparing the plots in the left and right columns in Figure 1, we see that although the real cluster data and the Gaussian ones exhibit certain discrepancies, they do not differ radically, and in any case they cannot be distinguished reliably only via such a comparison.

We then apply the Kolmogorov technique to the X-ray data for each cluster. Namely, we estimate the Kolmogorov stochasticity parameter $\lambda$ and the function $\Phi(\lambda)$ for the X-ray images, and do the same for the Gaussian images of each cluster. The maximal and minimal values of the resulting $\Phi$ functions are shown in Fig. 2 for all 40 clusters, as well as for their Gaussian mock clusters. We see that for real X-ray images of clusters the function $\Phi$ outside the center remains 1. On the other hand, its behavior for the Gaussian images is entirely different, i.e. far smaller at all radii. To test the dependence on the number of pixels in Fig. 3 we show these distributions for 4 clusters with large scatter in the pixel numbers: A0150 - 60; A3526 - 248; A0576 - 315; A2052 - 324. It is clear that, the higher is number of pixels, more outlined is the difference between the real clusters and the mock Gaussian ones.

---

[1]http://xmmssc-www.star.le.ac.uk/Catalogue/2XMM/

Table 1: Sample definition for the 40 clusters: running number, cluster name, redshift, galactic coordinates (of centers), number of pixels for which X-ray fluxes are given; the first 17 clusters have redshifts lower than 0.03, the others have a higher redshift.

| N | Abell | z | l, deg | b, deg | Pixel |
|---|-------|-----|--------|--------|-------|
| 1 | A0194 | 0.0178 | 141.95 | -63.00 | 97 |
| 2 | A0262 | 0.0151 | 136.59 | -63.00 | 183 |
| 3 | A0400 | 0.0232 | 170.53 | -44.90 | 116 |
| 4 | A1060 | 0.0114 | 269.64 | 26.51 | 85 |
| 5 | A1314 | 0.0323 | 151.84 | 63.57 | 86 |
| 6 | A1367 | 0.0208 | 234.81 | 73.03 | 102 |
| 7 | A1656 | 0.0219 | 58.09 | 87.96 | 758 |
| 8 | A2052 | 0.0338 | 9.40 | 50.10 | 324 |
| 9 | A2063 | 0.0341 | 12.86 | 49.81 | 99 |
| 10 | A2147 | 0.0338 | 28.81 | 44.49 | 45 |
| 11 | A2197 | 0.0296 | 64.82 | 43.80 | 45 |
| 12 | A2199 | 0.0309 | 62.90 | 43.70 | 103 |
| 13 | A2870 | 0.0225 | 294.81 | -69.95 | 73 |
| 14 | A2877 | 0.0235 | 293.14 | -70.88 | 169 |
| 15 | A3526 | 0.0102 | 302.42 | 21.56 | 248 |
| 16 | A3574 | 0.0148 | 317.47 | 30.94 | 162 |
| 17 | A3581 | 0.0218 | 323.13 | 32.85 | 285 |
| 18 | A0085 | 0.0543 | 115.06 | -72.06 | 83 |
| 19 | A0087 | 0.0538 | 116.01 | -72.55 | 100 |
| 20 | A0119 | 0.0430 | 125.76 | -64.11 | 159 |
| 21 | A0133 | 0.0554 | 149.10 | -84.09 | 77 |
| 22 | A0150 | 0.0576 | 129.62 | -49.47 | 60 |
| 23 | A0152 | 0.0569 | 129.71 | -48.65 | 65 |
| 24 | A0168 | 0.0438 | 136.67 | -62.04 | 127 |
| 25 | A0222 | 0.2110 | 162.67 | -72.20 | 217 |
| 26 | A0223 | 0.2070 | 162.42 | -72.00 | 217 |
| 27 | A0576 | 0.0381 | 161.42 | 26.24 | 315 |
| 28 | A1213 | 0.0468 | 201.46 | 68.99 | 94 |
| 29 | A1775 | 0.0705 | 31.93 | 78.71 | 73 |
| 30 | A1795 | 0.0619 | 33.79 | 77.16 | 265 |
| 31 | A1983 | 0.0424 | 18.95 | 60.12 | 113 |
| 32 | A2065 | 0.0714 | 42.88 | 56.56 | 98 |
| 33 | A2151 | 0.0354 | 31.60 | 44.52 | 112 |
| 34 | A2163 | 0.2005 | 6.76 | 30.52 | 143 |
| 35 | A2717 | 0.0478 | 349.21 | -76.48 | 145 |
| 36 | A3112 | 0.0738 | 252.94 | -56.08 | 88 |
| 37 | A3128 | 0.0587 | 264.74 | -51.11 | 111 |
| 38 | A3158 | 0.0585 | 256.06 | -48.92 | 78 |
| 39 | A3266 | 0.0577 | 272.19 | -40.15 | 393 |
| 40 | A4059 | 0.0463 | 356.84 | -76.06 | 113 |



Fig. 1: X-ray image of the cluster Abell 2870 obtained by XMM-Newton. The circle has a radius of 0.3°; the '0' of the scale bar below the figure corresponds to a flux of 41.3 in units of $10^{-15}$ erg cm$^{-2}$ s$^{-1}$, the minimal and maximal values of the bar are 7.3 and 405.6, respectively, in the same units.

randomly redistributed simulated Gaussian clusters. Although the original X-ray clusters and their simulated Gaussian versions do not show radically different behaviors in their flux distributions, a difference, however, is clearly outlined quantitatively in the behavior of the Kolmogorov function $\Phi$. For the real X-ray images of the clusters the function $\Phi$ tends to 1 outside the cluster cores, while for the Gaussian mock clusters it remains smaller at all radii.

Thus, the Kolmogorov method applied to X-ray images enables to distinguish a galaxy cluster from a random X-ray flux distribution, thus opening new possibilities in the detection of galaxy clusters.

REFERENCES

[1] KOLMOGOROV A.N., *G.Ist.Ital.Attuari,*, **4** (1933) 83
[2] ARNOLD V., *Nonlinearity*, **21** (2008) T109
[3] ARNOLD V.I., *Uspekhi Mat. Nauk*, **63** (2008) 5
[4] ARNOLD V.I., *Trans. Mosc. Math. Soc.*, **70** (2009) 31
[5] GURZADYAN V.G. & KOCHARYAN A.A., *A&A*, **492** (2008) L33; *A&A*, **493** (2008) L61
[6] GURZADYAN V.G., ALLAHVERDYAN A.E. *et al.*, *A&A*, **497** (2009) 343; *A&A*, **525** (2011) L7
[7] GURZADYAN V.G., KASHIN A.L. *et al.*, *EPL*, **91** (2010) 19001
[8] GURZADYAN V.G., ALLAHVERDYAN A.E., GHAHRAMANYAN T. *et al.*, *A&A*, **525** (2011) L7
[9] FERMI-LAT COLLABORATION, *arXiv:1002.2280*, (2010)
[10] FINOGUENOV A., HENRIKSEN, M.J., BRIEL U. G., DE PLAA J., KAASTRA J. S., *ApJ*, **611** (2004) 811
[11] DURRET F., LIMA NETO G.B., FORMAN W., *A&A*, **432** (2005) 809
[12] DURRET F., LIMA NETO, *AdSpR*, **42** (2008) 578
[13] BASILAKOS S., PLIONIS M., GEORGAKAKIS A. ET AL., *MNRAS*, **351** (2004) 989

**Conclusions.** – We analyzed a sample of 40 Abell X-ray clusters with available XMM-Newton data. By applying the Kolmogorov method to the X-ray data and to Gaussian simulated images, we revealed a clear difference in the behavior of Kolmogorov's function $\Phi$ for real clusters and for their Gaussian simulated images. The X-ray image of a real galaxy cluster carries correlations reflecting the gravitational potential of the cluster and hence, the physical conditions of the hot gas responsible for the X-ray emission. Such correlations are not present in the
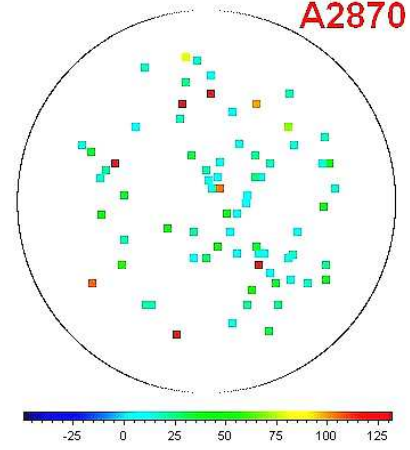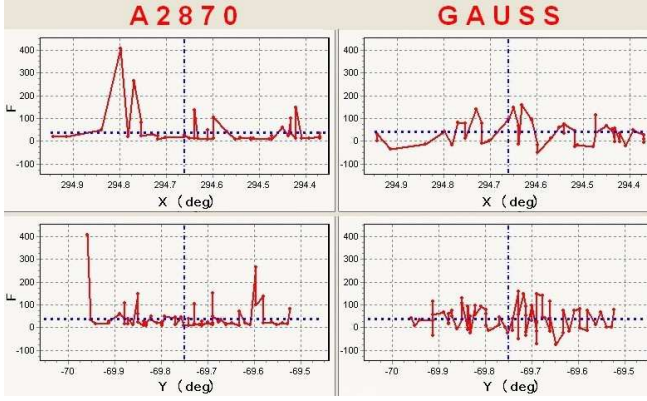
Fig. 2: Distribution of the pixel X-ray flux along the *l* (top) and *b* (bottom) axes for A2870 (left) and for the simulated Gaussian distribution of the X-ray data parameters (right).
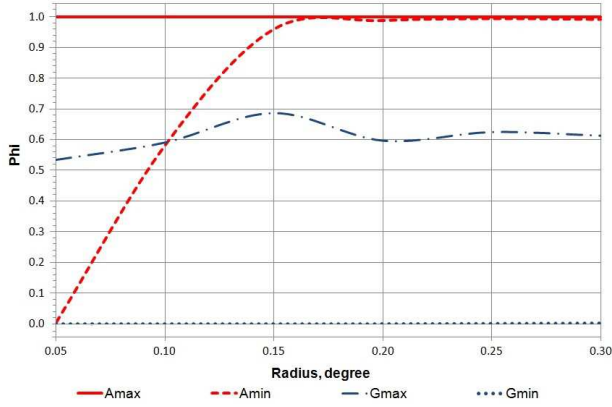
[14] Schwope A.D., Lamer G., Burke D. et al., *AdSpR*, **34** (2004) 2604

[15] Valtchanov I., Pierre M., Willis J. et al., *A&A*, **423** (2004) 75

[16] Williamson R., Benson B.A., High F.W. et al., *arXiv:1101.1290*, (2011)

[17] Aghanim N., Arnaud M., Ashdown M. et al., *arXiv:1101.2043*, (2011)

Fig. 3: Maximal and minimal values of the Kolmogorov function $\Phi$ vs the cluster radius (in degrees) for X-ray data for 40 galaxy clusters, as well as the same for corresponding Gaussian mock clusters (in blue).
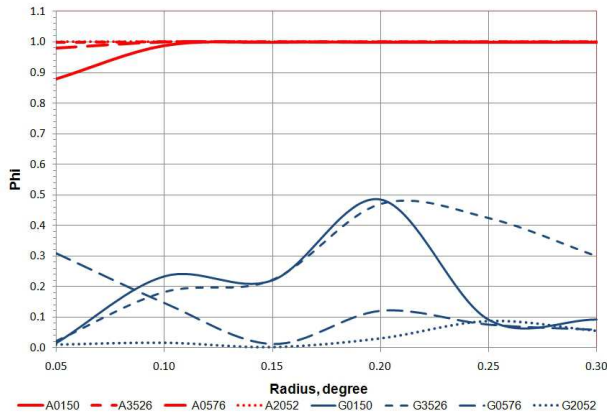


Fig. 4: Kolmogorov function vs the radius for 4 clusters with large scatter in the pixel numbers (along with their Gaussian versions): A0150 - 60; A3526 - 248; A0576 - 315; A2052 - 324.